Swift Observation of GRB 090423

H. A. Krimm (CRESST/GSFC/USRA), M. De Pasquale (MSSL/UCL), M. Perri (ASDC), G. Stratta (ASDC), T. N. Ukwatta (GSFC/GMU) for the Swift Team

1 Introduction

BAT triggered on GRB 090423 at 07:55:19 UT (Trigger 350184) (Krimm *et al.*, *GCN Circ.* 9198). This was an 1.024-sec rate-trigger on a intermediate length burst with $T_{90} = 10.3 \pm 1.1$ *sec*. Swift slewed to this burst immediately and XRT began follow-up observations at $T + 72.5$ *sec*, and UVOT at $T + 77$ *sec*. The best position is from NIR imaging with the WFCAM on UKIRT (Tanvir *et al.*, *GCN Circ.* 9202): RA($J2000$) = 148.888708° (09h 55m 33.29s), Dec($J2000$) = +18.149389° (+18°08′57″.8) with an error of 0.3 arcsec (estimated uncertainty).

No counterpart was detected in UVOT observations (see §4 for upper limits) or at any wavelength shorter than the J band (e.g. Cucchiara, Fox & Berger *GCN Circ.* 9209; Olivares *et al.*, *GCN Circ.* 9215). However, the source was detected in the J, H and K bands as well as at 3-mm (Castro-Tirado *et al.*, *GCN Circ.* 9273). This led Cucchiara, Fox & Berger (*GCN Circ.* 9209) to argue that the cut-off between the Y and J bands was a Lyman-α cutoff, suggesting that the burst was at redshift $z \sim 9$. Later photometry refined this redshift value, and Tanvir *et al.*(*GCN Circ.* 9219) detected a clear continuum at red wavelengths, but no flux below about 1120 nm, consistent with a break due to Lyman-α at a redshift $z \approx 8.2$. This burst represents the most distant GRB for which a spectroscopic redshift has been measured.

GRB 090423 was also detected by *Fermi*/GBM (von Kienlin, *GCN Circ.* 9229).

2 BAT Observation and Analysis

Using the data set from T-60 to T+243 sec, further analysis of GRB 090423 has been performed by the Swift/BAT team (Palmer et al., GCN 9204). The BAT ground-calculated position is RA, Dec = 148.891°, +18.165°, which is RA(J2000) = 09h 55m 33.8s Dec(J2000) = +18°09′55″.7 with an uncertainty of 1.1 arcmin, (radius, sys+stat, 90% containment). The partial coding was 92% (the bore sight angle was 25.0°).

The mask-weighted light curve (Figure 1) shows several overlapping peaks starting at ∼T-2 sec, peaking at ∼T+4 sec, and ending at ∼T+15 sec. T_{90} (15-350 keV) is 10.3 ± 1.1 sec (estimated error including systematics).

The time-averaged spectrum from T-0.7 to T+11.7 sec is best fit by a power law with an exponential cutoff. This fit gives a photon index 0.80 ± 0.50, and E_{peak} of 48.6 ± 6.2 keV ($\chi^2 = 41.4$ for 56 d.o.f.). The fluence in the 15-150 keV band is $5.9 \pm 0.4 \times 10^{-7}$ *erg cm*$^{-2}$. The 1-sec peak photon flux measured from T+3.50 sec in the 15-150 keV band is 1.7 ± 0.2 *ph cm*$^{-2}$ *s*$^{-1}$. A fit to a simple power law gives a photon index of 1.90 ± 0.10 ($\chi^2 = 59.9$ for 57 d.o.f.). All the quoted errors are at the 90% confidence level.

Using the Swift/BAT data we have completed spectral lag analysis for GRB 090423 (Krimm *et al.*, *GCN Circ.* 9241). Using 16-ms binning on the event data, for the "whole" burst (15 seconds), we obtain:

chans $3 \rightarrow 1 : 0.046^{+0.085}_{-0.058}$ *sec*

chans $3 \rightarrow 2 : 0.044^{+0.070}_{-0.052}$ *sec*

For the peak 3 seconds of the burst we obtain:

chans $3 \rightarrow 1 : 0.021^{+0.054}_{-0.032}$ *sec*

chans $3 \rightarrow 2 : 0.006^{+0.046}_{-0.071}$ *sec*

where the channels are 15-25 keV, 25-50 keV, and 50-100 keV. The lag in each case is consistent with zero, but the 1σ error bars are roughly as large as the median lag values for long bursts. Thus this burst is too dim for us to utilize lags as a discriminant for long vs. short.

Given the relatively short duration of this burst, it is informative to look at other possible indicators of whether the burst is in fact a short burst seen at a large distance.

The calculations below use z=8, which is roughly the average of the photometric and spectroscopic redshifts determined for this burst (Cucchiara *et al.*, *GCN Circ.* 9213; Olivares *et al.*, *GCN Circ.* 9215; Thoene *et al.*, *GCN Circ.* 9216; Perley *et al.*, *GCN Circ.* 9217; Tanvir *et al.*, *GCN Circ.* 9219; Fernandez-Soto *et al.*, *GCN Circ.* 9222).

When converted to the rest frame, the T_{90} values (*Swift*/BAT: 10.3 ± 1.1 sec) and (*Fermi*/GBM: 12 sec, (8-1000 keV), Kienlin *GCN Circ.* 9229) transform to 1.1 ± 0.1 sec and 1.3 sec, respectively. However, one must be careful in comparing these numbers to the BATSE short-hard burst divide (Kouveliotou et al., ApJ **413**, L101, 1993). The BATSE duration distribution is in the observer frame. With a typical redshift of z = 1-2 for BATSE bursts, the dividing line between long and short in the rest frame is 0.7 to 1.0 seconds. Thus this burst is on the boundary and toward the long side.

While the duration and lag are consistent with short bursts (with large errors), there are other observations which are more consistent with GRB 090423 being a long burst in the source frame.

The spectral fits to the BAT data are inconclusive as to whether this is a long or short burst. Both the photon index, $\alpha = 0.8 \pm 0.5$, and $E_{peak} = 440$ keV in the source frame, from a cut-off power-law model fit, are consistent with the results for other short bursts detected by Swift/BAT. However, these numbers also fall within the distributions for long bursts (Krimm et al., submitted to ApJ).

The main argument against this being a short burst is the isotopic energy. The analysis performed by Amati *et al.*, (*GCN Circ.* 9227) gives the burst $E_{iso} = 10^{53}\ erg$ and shows that the burst is consistent with the $E_{peak} - E_{iso}$ relation for long bursts. All previously known short bursts are outliers to this relation. The calculated value of E_{iso} is a factor of > 50 greater than that for most other short bursts.

In conclusion, we can not say if GRB 090423 is short or long. Its duration in the source frame is at the boundary between the two classes, the lag analysis is inconclusive, the BAT spectral shape is inconclusive, the Amati relationship favors long burst and the merger time at such high redshift could be problematic for a short burst interpretation.

3 XRT Observations and Analysis

Using the 8.08 ks of XRT data of GRB 090423 in Photon Counting (PC) mode), the enhanced XRT position (using the XRT-UVOT alignment and matching UVOT field sources to the USNO-B1 catalogue) is RA($J2000$) = 148.88825° (09h 55m 33.18s), Dec($J2000$) = +18.14925° (+18°08′57″.3) with an uncertainty of 1.4 arcsec (90% confidence, including boresight uncertainties). This is consistent with the optical position found by Tanvir *et al.*, *GCN Circ.* 9202.

The $0.3 - 10\ keV$ light curve (Fig 3) during the first *Swift* orbit shows a flare peaking at T+170 s (Stratta & Perri *GCN Circ.* 9212). There is a hint of this flare in the BAT light curve (Fig. 2). Starting from the second orbit (T+3.9 ks) the curve is well described by a power-law model with index $\alpha = -1.36 \pm 0.06$. The decay was steady until T+676 ks, when the source became moon constrained and observations were terminated.

The X-ray spectrum during the power-law decay is well fit by an absorbed power-law model with a photon index of $\Gamma = 2.0 \pm 0.1$ and a total column density of $n_H = (8.7 \pm 2.5) \times 10^{20}\ cm^{-2}$. The Galactic column density in the direction of the source is $2.9 \times 10^{20}\ cm^{-2}$ (Kalberla et al. 2005). The counts to observed (unabsorbed) 0.3-10 keV flux conversion factor deduced from this spectrum is

$3.7 \times 10^{-11} (4.6 \times 10^{-11})$ $erg\ cm^{-2} count^{-1}$. Errors are given at the 1σ level.

4 UVOT Observation and Analysis

After analysis of Swift Ultraviolet/Optical Telescope (UVOT) data of GRB 090423 (De Pasquale & Krimm, GCN 9210), starting 77 sec after the BAT trigger, there is no detection of any source at the enhanced Swift XRT position nor at the position of the K band candidate found by UKIRT (Tanvir *et al.*, *GCN Circ.* 9202). No source is detected even when all the images of all filters are summed. The 3σ upper limits for detecting a source in the white and u band first exposures, and subsequent co-added images in all filters are:

Filter	Start	Stop	Exposure	Magnitude
white	77	227	147	> 20.7
u	290	540	246	> 20.0
v	619	6162	413	> 19.6
b	545	5497	413	> 20.2
u	290	5342	462	> 20.4
uvw1	668	6503	344	> 20.1
uvm2	644	6367	413	> 20.1
uvw2	594	5958	412	> 20.5
white	77	5752	560	> 21.3

Table 1: Magnitude limits from UVOT observations.

The quoted upper limits have not been corrected for the expected Galactic extinction along the line of sight of $E_{B-V} = 0.03$ mag (Schlegel *et al.*, 1998, ApJS **500**, 525). All photometry is on the UVOT photometric system described in Poole *et al.*, (2008, MNRAS **383**, 627).

In Fig. 4 we show a summed exposure, made up of all the white filter exposures available. Our white filter 3σ upper limit, including all data, is now $m_{\rm white} > 23.6$.

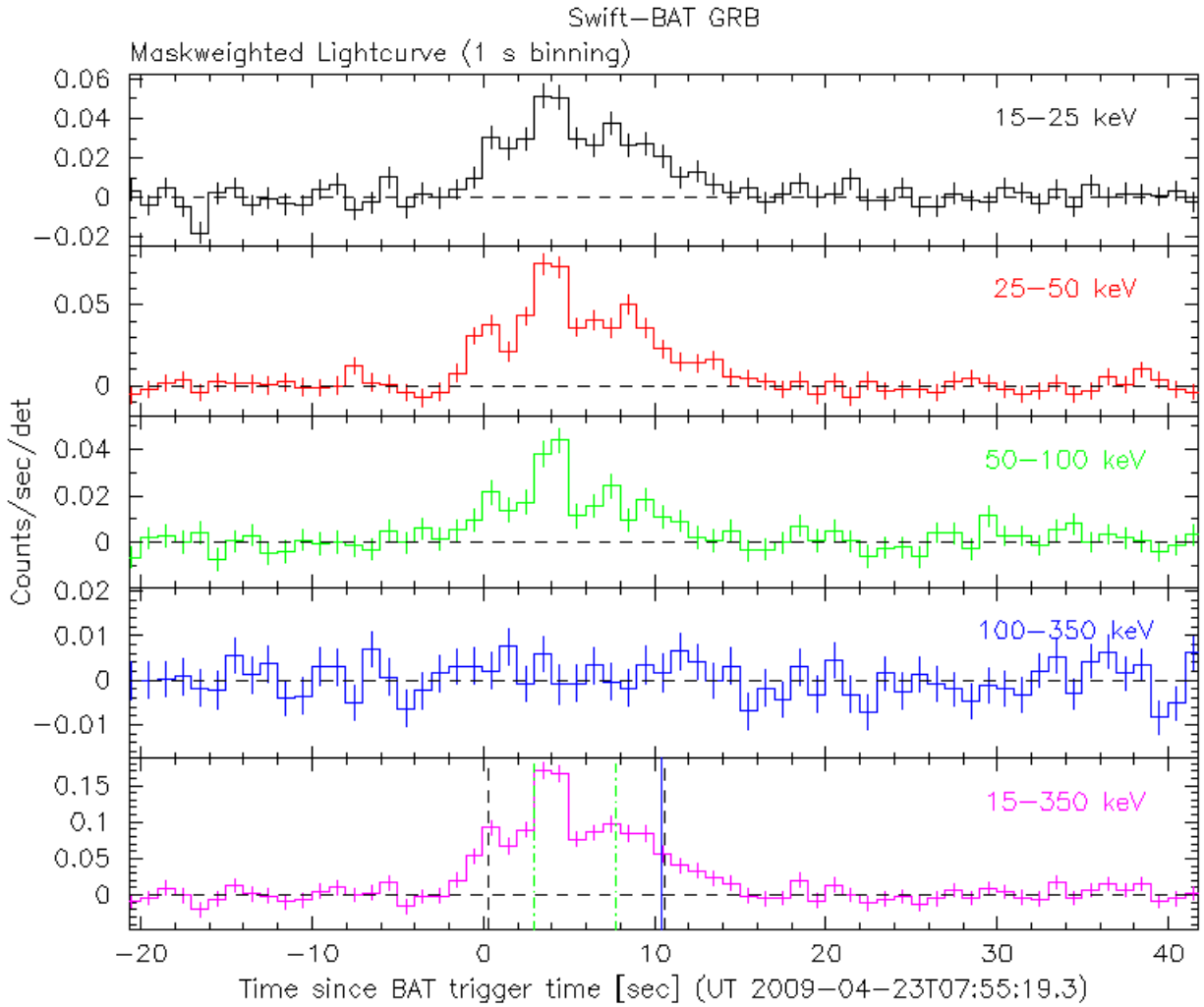

Figure 1: BAT Light curve. The mask-weighted light curve in the 4 individual plus total energy bands. The units are counts/sec/illuminated-detector (note illum-det = 0.16 cm^2).

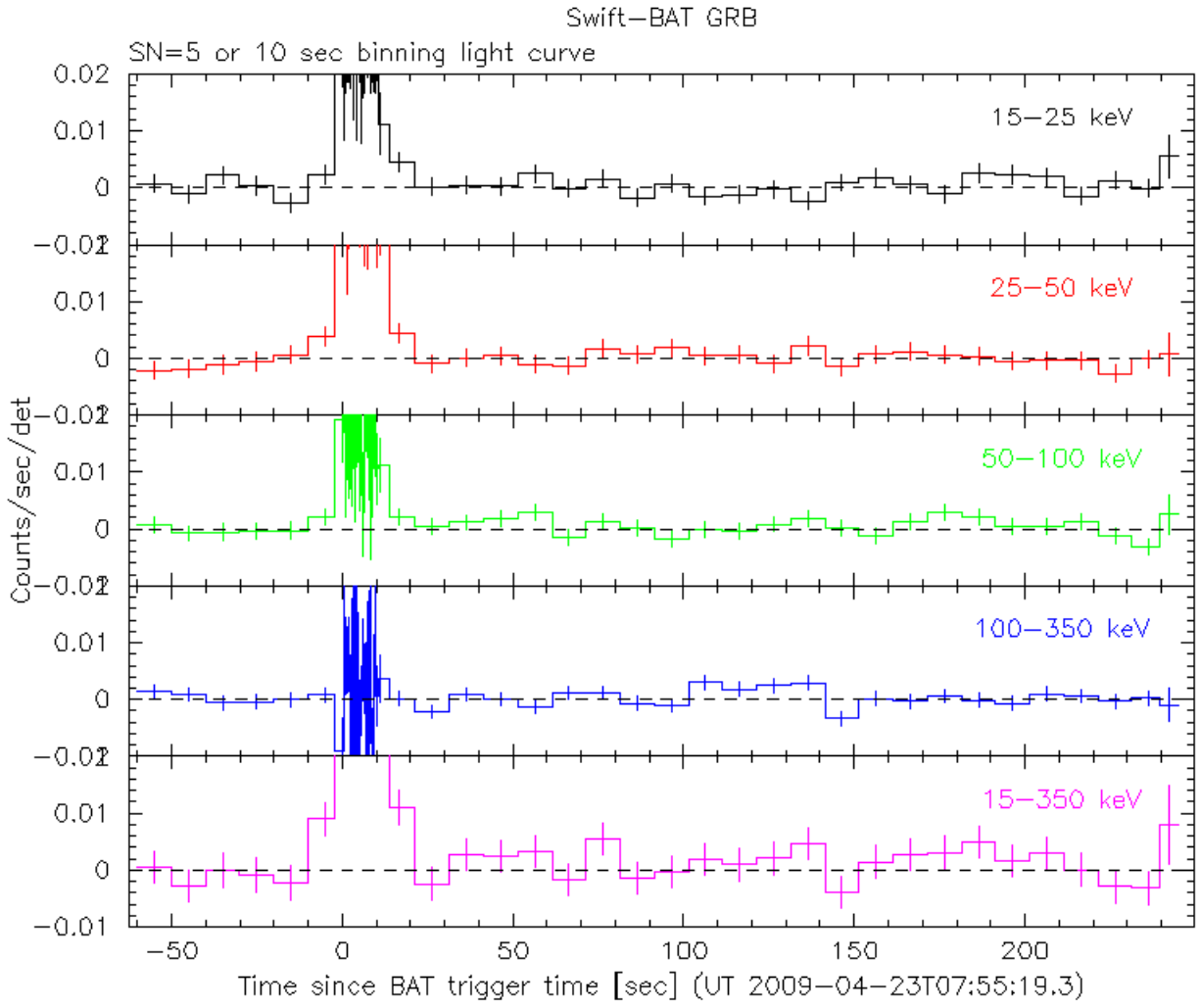

Figure 2: BAT Light curve. The extended mask-weighted light curve binned to emphasize late low-level emission. The units are counts/sec/illuminated-detector (note illum-det = 0.16 cm^2).

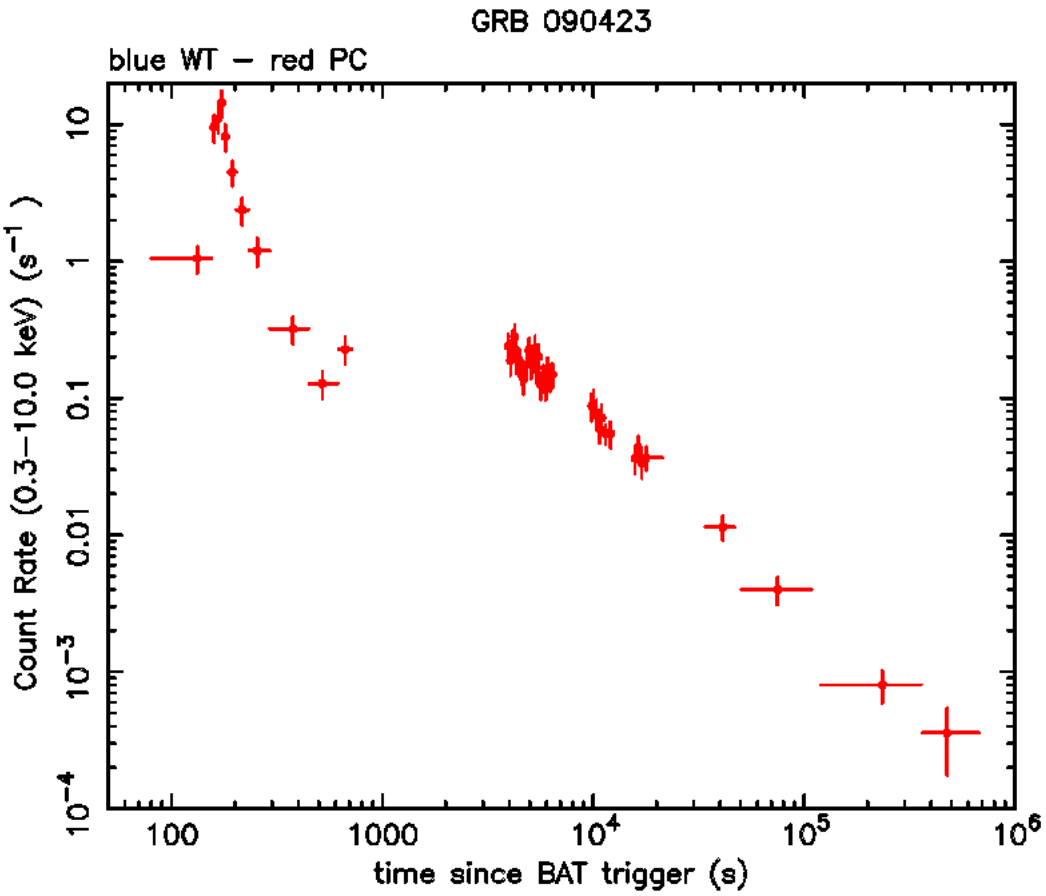

Figure 3: XRT light-curve. Counts s^{-1} in the 0.3-10 keV band for the Photon Counting mode (red). The approximate conversion of the 0.3 – 10 keV observed flux is 1 count $s^{-1} \sim 3.7 \times 10^{-11} erg\ cm^{-2} s^{-1}$.

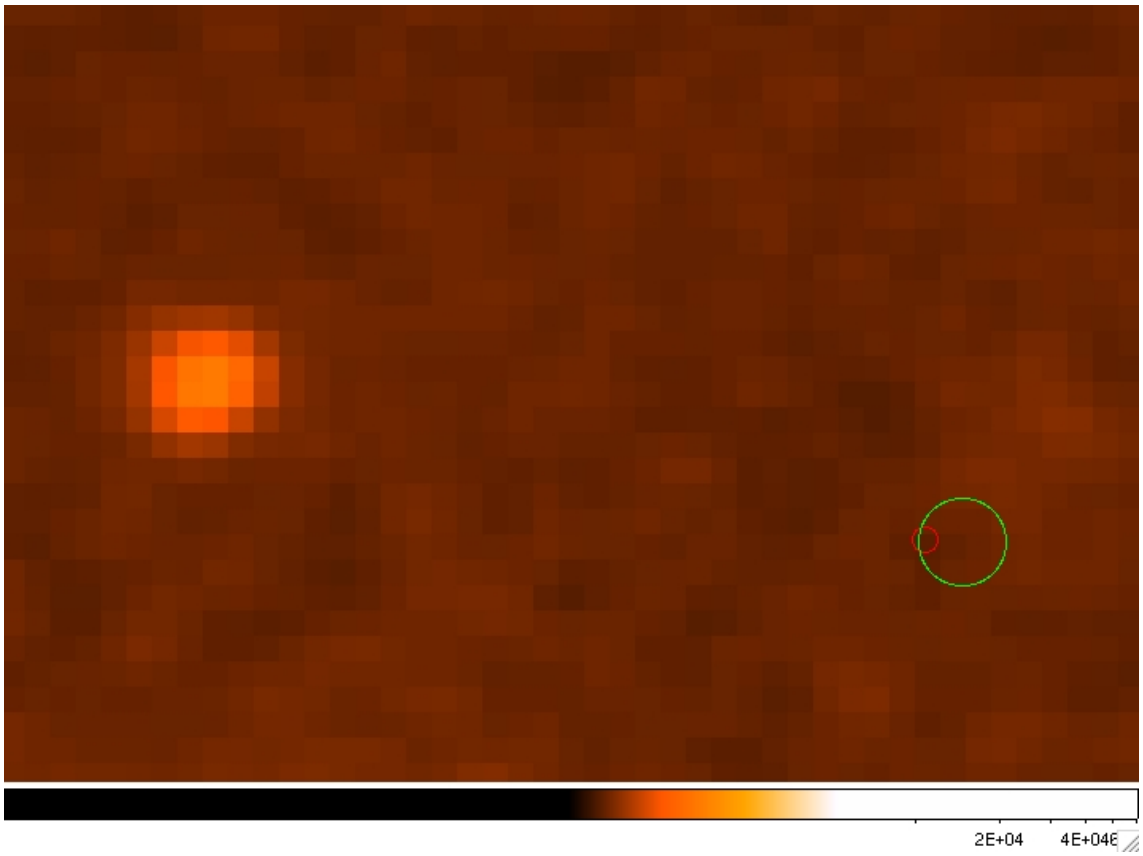

Figure 4: Summed UVOT exposure, made up of all the white filter exposures available. The exposure includes observations from T+77 – T+600,200 s. The exposure time is 13 ks. The green circle is the refined XRT error circle, with a radius of 1.7″. The red circle flags the position of the source found by Tanvir *et al.*, *GCN Circ.* 9202, and confirmed to be the optical afterglow of this burst.